UC Irvine
UC Irvine Previously Published Works

Title
Fabrication and characterization of biomimetic multichanneled crosslinked-urethane-doped polyester tissue engineered nerve guides

Permalink
https://escholarship.org/uc/item/52k8p31f

Journal
Journal of Biomedical Materials Research Part A, 102(8)

ISSN
1549-3296

Authors
Tran, Richard T
Choy, Wai Man
Cao, Hung
et al.

Publication Date
2014-08-01

DOI
10.1002/jbm.a.34952

Peer reviewed

eScholarship.org Powered by the California Digital Library
University of California

NIH Public Access
Author Manuscript
J Biomed Mater Res A. Author manuscript; available in PMC 2015 August 01.

Published in final edited form as:
J Biomed Mater Res A. 2014 August ; 102(8): 2793–2804. doi:10.1002/jbm.a.34952.

Fabrication and characterization of biomimetic multichanneled crosslinked-urethane doped polyester (CUPE) tissue engineered nerve guides

Richard. T. Tran[1], **Wai Man Choy**[2], **Hung Cao**[3], **Ibrahim Qattan**[4], **Jung-Chih Chiao**[3], **Wing Yuk Ip**[2,*], **Kelvin Wai Kwok Yeung**[2,*], and **Jian Yang**[1,*]

[1]Department of Bioengineering, Materials Research Institute, The Huck Institutes of the Life Sciences, The Pennsylvania State University, University Park, PA 16802, USA

[2]Department of Orthopaedics and Traumatology, Queen Mary Hospital, The University of Hong Kong, Hong Kong SAR

[3]Department of Electrical Engineering, The University of Texas at Arlington, Arlington, TX 76010, USA

[4]Department of Bioengineering, The University of Texas at Arlington, Arlington, TX 76010, USA

Abstract

Biomimetic scaffolds that replicate the native architecture and mechanical properties of target tissues have been recently shown to be a very promising strategy to guide cellular growth and facilitate tissue regeneration. In this study, porous, soft, and elastic crosslinked urethane-doped polyester (CUPE) tissue engineered nerve guides were fabricated with multiple longitudinally oriented channels and an external non-porous sheath to mimic the native endoneurial microtubular and epineurium structure, respectively. The fabrication technique described herein is highly adaptable and allows for fine control over the resulting nerve guide architecture in terms of channel number, channel diameter, porosity, and mechanical properties. Biomimetic multichanneled CUPE guides were fabricated with various channel numbers and displayed an ultimate peak stress of 1.38 ± 0.22 MPa with a corresponding elongation at break of 122.76 ± 42.17 %, which were comparable to that of native nerve tissue. The CUPE nerve guides were also evaluated *in vivo* for the repair of a 1 cm rat sciatic nerve defect. Although histological evaluations revealed collapse of the inner structure from CUPE TENGs, the CUPE nerve guides displayed fiber populations and densities comparable with nerve autograft controls after 8 weeks of implantation. These studies are the first report of a CUPE-based biomimetic multichanneled nerve guide and warrant future studies towards optimization of the channel geometry for use in neural tissue engineering.

Keywords

biomimetic; biodegradable elastomer; multichanneled scaffold; nerve guide; tissue engineering

[*]Corresponding authors: J. Yang; jxy30@psu.edu, W.Y. Ip; wyiphkucc@yahoo.com.hk, K.W.K. Yeung; wkkyeung@hku.hk.

NIH-PA Author Manuscript
NIH-PA Author Manuscript
NIH-PA Author Manuscript

NIH-PA Author Manuscript

NIH-PA Author Manuscript

NIH-PA Author Manuscript

INTRODUCTION

Peripheral nerves have an intrinsic capacity to regenerate following injury. When the nerve defect or “gap” length is smaller than a few millimeters, the damaged proximal stump is able to regenerate axonal sprouts towards the distal segment to re-establish both motor and sensory function.[1,2] However, peripheral nerves severed beyond the point of repair necessitate surgical intervention primarily in the form of a nerve autograft, which relies on the premise that viable Schwann cells located in the basal lamina tubes release a synergistic combination of growth factors and cell adhesion molecules to support and direct oriented axonal regeneration.[3,4] Unfortunately, this form of neural regeneration is associated with many disadvantages including the need for multiple surgical procedures, limited availability of suitable grafts, loss of function at the donor site, and potential for neuroma formation.[2,5-7] More importantly, the use of a nerve autograft does not always result in full functional recovery with only 50% of patients regaining useful function due to the misdirection of the regenerating axons or inappropriate target reinnervation.[5,8]

Attempts in creating suitable alternatives to address the limitations associated with the use of nerve autografts has produced a wide array of tissue engineered nerve guides (TENGs) to bridge the transected nerve.[7] An assortment of biomaterials such as collagen,[9] poly (L-lactide),[10] polyamides,[11] poly (phosphoesters),[12] and poly (ethylene)[13] have been used in combination with numerous processing techniques to fabricate synthetic alternatives, which can provide a physical substrate for the regenerating neural defect.[14] Due to the ease of manufacturing, many of the previous TENG designs have been predominantly based upon the entubulation model where the proximal and distal stumps of the damaged nerve are inserted into either end of a porous foam rod or hollow tube to induce fibrin matrix production in an oriented direction.[15,16] Unfortunately, the use of a single hollow guide is not optimal for nerve regeneration due to the limited available surface area for cell growth and the inability to recreate the proper native spatial arrangement of the extracellular matrix and cells within the conduit.[6] To overcome these limitations, recent years have witnessed the development of increasingly sophisticated and biomimetic TENGs microfabricated for improved function based upon the mechanisms of contact guidance and basement membrane microtube theory, which hypothesize that axon elongation requires guidance by contact with the appropriate substrate through topographical control. For example, longitudinally oriented channels have been introduced into TENGs to better recreate the highly oriented architecture needed for appropriate cellular alignment and promote the body’s natural pattern of growth.[7,17-19] In addition to being architecturally biomimetic, these multichanneled TENG designs are also advantageous in that they provide improved nerve target reinnervation, a greater surface area for cell growth allowing for denser populations, and internal support for improved mechanical strength.[5,7,8,20-22]

Thus, in order to produce a successful “off-the-shelf” TENG and to move research closer to clinical application, we set out to develop a novel scaffold that is 1) architecturally biomimetic to allow for adequate cell densities and promote cellular alignment along the length of the guide, 2) highly porous to assist in cell-cell communication and facilitate nutrient, metabolite, and waste exchange through an open and interconnected structure, 3) mechanically compliant to mimic the softness and elasticity of native nerve tissues in a

NIH-PA Author Manuscript

NIH-PA Author Manuscript

NIH-PA Author Manuscript

dynamic environment, 4) fabricated using transferable fabrication methods that are relatively cost-effective and can be easily applied to a wide variety of materials to fit a particular application, and 5) biocompatible and biodegradable in order to minimize the host inflammatory response and be resorbed by the body at the rate of neo-tissue formation, respectively. To test the above hypotheses, the purpose of this study is to fabricate and characterize porous multichanneled TENGs fabricated from crosslinked urethane-doped polyester (CUPE), which is a biocompatible, soft, and highly elastic material previously developed for vascular applications.[23] The biomimetic multichanneled CUPE TENGs were characterized for their resulting geometries, mechanical strength, and *in vivo* to repair a 1 cm rat sciatic nerve defect.

MATERIALS AND METHODS

All chemicals were purchased from Sigma-Aldrich (St. Louis, MO, USA), unless mentioned otherwise, and used as received.

Crosslinked urethane-doped polyester pre-polymer (pre-CUPE) synthesis

Pre-CUPE was synthesized in two distinct steps similar to previously published methods.[23] The first step involves the formation of a low molecular weight citric acid-based pre-polymer soft segment, poly (octanediol citrate) (pre-POC), which is later chain extended by 1,6-hexamethyl diisocyanate (HDI) in the final urethane-doping reaction. Pre-POC was synthesized by melting a 1.0:1.1 molar feeding ratio of citric acid and 1,8-octanediol, respectively, at 160 °C in a three-necked round bottom flask fitted with an inlet and outlet adapter under a constant flow of nitrogen while stirring. Once all the monomers had melted, the temperature of the system was reduced to 140 °C, and the reaction mixture was allowed to proceed for 60 minutes. The resulting mixture was purified by drop-wise precipitation in deionized water, collected, and lyophilized for 48 hours to obtain the final POC pre-polymer. In the second urethane-doping step, pre-POC chain extension was achieved by dissolving the purified pre-POC in 1,4-dioxane to form a 3.0 % solution by weight, and reacted with HDI under constant stirring at 55 °C using stannous octoate as a catalyst (0.1 wt.-%). Complete diisocyanate reaction to pre-POC was confirmed upon the disappearance of the isocyanate peak located at 2267 cm^{-1} of Fourier-transform infrared (FT-IR) analysis using a Nicolet 6700 FT-IR spectrometer (Thermo Fisher Scientific, Waltham, MA, USA). In this study, pre-POC was reacted with HDI in 1.0:1.2, 1.5, or 1.8 molar ratios of pre-POC and HDI, respectively, to determine the effects of urethane doping amounts on the resulting scaffold mechanical strength.

Multichanneled TENG fabrication

Porous CUPE multichanneled TENGs were fabricated according to the schematic illustrated in Figure 1. First, 127 μm thick titanium shims (Fig. 1A) were made using a programmable 355 nm 5 W Oxford Laser Micromachining System (Oxford Lasers, Inc., Shirley, MA, USA). The design was sketched by Alphacam Software (Planit Americas, Tuscaloosa, AL, USA), and translated into a G-code program. A layer of photoresist was coated on the titanium piece before machining to protect the samples. After cutting, the molds were cleaned by acetone to remove the photoresist and debris. Next, combinations of 5-500 μm

NIH-PA Author Manuscript

NIH-PA Author Manuscript

NIH-PA Author Manuscript

diameter steel acupuncture needles (Lhasa OMS, Inc., Weymouth, MA, USA) were inserted through two titanium shims (Fig. 1B). A pre-CUPE solution was mixed with sodium chloride salt with an average size in the range of 1-10 μm in a 1:5 polymer to salt ratio by weight, respectively, and cast in between the acupuncture needles (Fig. 1C). After drying overnight in a laminar flow hood, the scaffolds were dip-coated with a separate pre-CUPE solution to form a non-porous outer sheath (Fig. 1D). To crosslink the pre-polymer, the guides were post-polymerized in an oven for predetermined times, X-Y, where X denotes the post-polymerization temperature and Y denotes the post-polymerization time in days (Fig. 1E). For example, 80-2 indicates that the guides were post-polymerized at 80 °C for 2 days, and 80-4 + 120-1 indicates that the guides were post-polymerized at 80 °C for 4 days followed by an additional day at 120 °C. Salt was leached out from the guides by immersion in deionized water for 72 hours with water changes every 12 hours (Fig. 1F). The acupuncture needles were removed by swelling the guides in 50% ethanol followed by lyophilization for 36 hours to remove any residual water.

Multichanneled CUPE TENG morphology and porosity characterization

Titanium shims were examined under a Hitachi S-3000N scanning electron microscope (SEM) (Hitachi, Pleasanton, CA, USA) to view hole diameters. To view the guide cross-sectional morphology, samples were freeze-fractured using liquid nitrogen, sputter coated with silver, and viewed under SEM. To characterize the shim and guide geometries, 3 random locations were selected and a total of 30 measurements were recorded using NIH Image J analysis software. The guide porosity was measured using the Archimedes' Principle similar to previously published methods.[24] A density bottle was used to measure the density and porosity of the guides using ethanol (density ρ_e) as the displacement liquid at 30 °C. First, the density bottle filled with ethanol was weighed (W_1). A sample (without the non-porous outer sheath) of weight (W_S) was immersed into the density bottle, and the air trapped in the sample was evacuated under vacuum. Next, the density bottle was supplemented with ethanol, filled, and weighed (W_2). The ethanol-saturated sample was removed from the density bottle, and the density bottle was weighed (W_3). The following parameters of the sample were calculated: the volume of the guide pore (V_P), the volume of the guide skeleton (V_S), the density (ρ_S), and the porosity (ε). The following formulas for the volume-mass index (V_P/V_S) were used:[24]

$$\begin{aligned} V_p &= (W_2 - W_3 - W_S)/\rho_e \\ V_S &= (W_1 - W_2 + W_S)/\rho_e \\ \rho_S &= W_S/V_S = W_S\rho_e/(W_1 - W_2 + W_S) \\ \varepsilon &= V_P/(V_P + V_S) = (W_2 - W_3 - W_S)/(W_1 - W_3) \end{aligned}$$

Multichanneled CUPE TENG mechanical characterization

Tensile mechanical testing was conducted according to ASTM D412A standard on a MTS Insight 2 fitted with a 10 N load cell (MTS, Eden Prairie, MN, USA). Briefly, complete porous multichanneled TENGs (with solid outer sheaths) of 10 mm lengths were pulled at a rate of 500 mm min^{-1} and elongated to failure. Values were converted to stress-strain and the initial modulus was calculated from the initial gradient of the resulting curve (0-10% elongation). The peak stress (MPa) and maximum elongation at break (%) were recorded.

NIH-PA Author Manuscript

NIH-PA Author Manuscript

NIH-PA Author Manuscript

The suture retention strength was obtained similar to previously reported methods.[25] Briefly, one end of a sample (10 mm length) was fixed with the stage clamp of the mechanical tester, and the other end was connected to the opposite clamp through the suture (5-0 Prolene, Ethicon, Piscataway, NJ, USA). The suture was placed 2 mm from the end of the sample. The measurement was performed using a 10 N load cell, and pulled at a rate of 8 mm min^{-1} until failure. The maximum load at rupture was recorded (N).

Multichanneled CUPE TENG *in vivo* evaluation

Lewis rats (3 months old; 300-350 g in weight) from the Laboratory Animal Unit of The University of Hong Kong were used to evaluate the porous multichanneled TENGs' ability to regenerate peripheral nerves *in vivo*. The rats were housed in The University of Hong Kong's Laboratory Animal Unit (LAU) with 12-hour light/dark cycles and free access to food and water. The University of Hong Kong Ethics Committee and The Department of Health of Hong Kong Licensing Office reviewed and approved all the protocols in this study. All rats were randomized for three studies. Animals were anesthetized 30 minutes before the operation by a mixture of Ketamine (20 mg kg^{-1}) and Xylazine (2.0 mg kg^{-1}) in a 10:1 ratio through intra-muscular injection. Temgesic (0.05 mg kg^{-1}) and Terramycin (60 mg kg^{-1}) were also injected subcutaneously to relieve any pain. The operation sites were located on the right side of hind legs, which were shaved and disinfected with 0.5% chlorhexidine. An incision was made from the rat's midline to the tibiofemoral articulation. The sciatic nerve from the right hind leg was dissected free from the surrounding tissues. After the right sciatic nerve was exposed, a one centimeter long nerve was transected and followed by the immediate replacement with the following grafts: 1) biomimetic multichanneled CUPE TENGs (CUPE with HDI ratio of 1.5 crosslinked at 80-4 + 120-1), 2) poly (caprolactone) (PCL) hollow tubes, and 3) nerve autografts, which were reversed 180° and implanted as a control. Following the surgical procedure, the wound was sutured and dressed by a marcaine block. After the operation, a three-day course of Ketoprofen (5.0 mg kg^{-1}) and Temgesic (0.05 mg kg^{-1}) was injected subcutaneously for pain relief. The rats also received 1.0 mg kg^{-1} terramycin (antibiotics) for four days post-operation.

After eight weeks of implantation, the rats were euthanized by an overdose sodium pentobarbital solution. The sciatic nerves from the operated side were harvested and separated into five sections: 1) proximal nerve, 2) proximal conduit, 3) central conduit, 4) distal conduit and 5) distal nerve. The explanted tissues were fixed in 4.0% paraformaldehyde overnight and embedded in paraffin. Semi-thin sections (7.0 μm) of nerve explants were sectioned and stained with hematoxylin and eosin (H&E) and toluidine blue staining. Toluidine blue stains axon myelin and does not react with CUPE. The resulting sections were placed on the stage of an inverted microscope and viewed under light microscopy (Nikon, Melville, NY, USA) and digitally recorded using a CCD camera. To characterize the sample morphology, nerve fiber population, area, density, and diameter of myelinated fibers, sections from the central conduit were analyzed using NIS-Elements Imaging Software (Nikon, Melville, NY, USA). The number of axons were counted using toluidine blue stained sections to give the number of axons, which were normalized to the image area dimension (# axons counted/0.0111 mm^2). The area of each axon was measured,

NIH-PA Author Manuscript

NIH-PA Author Manuscript

NIH-PA Author Manuscript

summed, and expressed as total axon area/image area to give the nerve fiber density. For each sample, six random areas from five cross-sections were evaluated.

Statistical analysis

Data was expressed as the means ± standard deviation (n = 6). The statistical significance between two sets of data was calculated using a two-tail Student's t-test. Non-parametric one-way ANOVA tests were also performed where appropriate. Data was taken to be significant when a $p < 0.05$ was obtained.

RESULTS

Multichanneled CUPE TENG fabrication

CUPE pre-polymers of various urethane-doping concentrations (HDI ratios of 1.2, 1.5, and 1.8 to 1.0 mole of POC) were successfully synthesized and used to fabricate multichanneled TENGs using a negative replica molding technique. The overall diameter of computer-aided design titanium shims was verified by ImageJ Analysis Software to be 2.55 ± 0.05 mm composed of 5 micro-machined 539.38 ± 8.57 μm holes (Figs. 2A and 2B). A total of 2 shims per guide were used to dictate the spatial orientation and dimensions of the acupuncture needles, which are used to form the guide channels (Fig. 1A). After casting the pre-polymer/salt slurry in between the acupuncture needles and allowing for complete solvent evaporation, the hardened polymer/salt mixture was then dip-coated in a separate CUPE pre-polymer solution to successfully form a non-porous outer sheath to surround the porous multichanneled region (Fig. 1D). Polymer crosslinking was successfully achieved through a controlled post-polymerization step (Fig. 1E), and the resulting TENG was soft, elastic, and composed of evenly spaced longitudinally oriented channels (Fig. 2C). The cross-sectional geometry of the guides was circular with slight irregularities in the porous phase of the guide (Fig. 2C). Figure 2D show the elastic nature of the CUPE TENG, as bending over 180° and applied force with multiple angles did not result in conduit kinks.

Multichanneled CUPE TENG morphology and porosity characterization

Representative SEM images of the overall architecture of the CUPE TENGs are shown in Figures 3 and 4. The overall diameter of the guides was determined using ImageJ Analysis Software and measured to be 2.99 ± 0.23 mm, which was primarily dictated by the titanium shim diameter and number of coats during sheath incorporation. The non-porous outer sheath thickness was measured to be 232.55 ± 48.10 μm, and the inner diameter of the conduits was measured to be 2.26 ± 0.11 mm (Fig. 3A). Figure 3B shows representative SEM images of the porous internal structure between each channel. The porous internal structures were composed of pores 12.14 ± 6.94 μm in diameter with a corresponding porosity of 67.52 ± 6.27 %. Although the presence of dead pores was visible in certain areas, the majority of pores were interconnected as shown in Figure 5B. Interestingly, submicron porosity was also observed on the luminal surface of the channels (Fig. 3C). Individual channel diameters were measured to be 515.24 ± 19.03 μm and similar in diameter to the acupuncture needles used during fabrication (Fig. 3D). Figure 4 shows representative SEM images of various guides of 1-5 channels fabricated using a single machined mold design.

NIH-PA Author Manuscript

NIH-PA Author Manuscript

NIH-PA Author Manuscript

Multichanneled CUPE TENG mechanical characterization

The fabricated multichanneled CUPE TENGs were evaluated for their tensile peak stress, initial modulus, elongation at break, and suture retention strengths. CUPE synthesized with a 1.2 HDI ratio was used for scaffold fabrication and crosslinked at various post-polymerization conditions to determine the effects of the extent of polymer crosslinking on the resulting mechanical properties and suture retention strength (Figs. 5A-C). As shown in Figure 5A, an increasing trend in peak stress and initial modulus was seen as the CUPE crosslinking time and temperature was increased. When compared to guides post-polymerized at 80 °C for 2 days (80-2), CUPE TENGs of similar chemical composition crosslinked at 80 °C for 4 days followed by 120 °C for one day (80-4 + 120-1) resulted in a significant increase tensile peak stress from 0.97 ± 0.12 MPa to 1.38 ± 0.22 MPa (Fig 5A), initial modulus of 0.64 ± 0.06 MPa to 1.01 ± 0.15 MPa (Fig 5A), and suture retention strengths of 1.49 ± 0.13 N to 2.36 ± 0.11 N (Fig 5C) ($p < 0.01$). As shown in Figure 5B, the same increase in polymer crosslinking also showed a significant reduction in elongation at break from 318.44 ± 12.59% down to 122.76 ± 42.12% ($p < 0.01$). The effect of CUPE HDI ratio on the resulting guide mechanical properties was also evaluated. The mechanical properties of multichanneled TENGs fabricated from CUPE of 1.2, 1.5, and 1.8 HDI ratios held at the same crosslinking condition (80-4 + 120-1) are shown in Figures 5D-5F. Similar to increasing the polymer crosslinking temperature and duration, an increase in urethane-doping amounts resulted in an increase in guide peak stress, initial modulus, and suture retention strengths. However, unlike increased polymer crosslinking, an increase in CUPE HDI ratio resulted in a corresponding increase in elongation at break. Increasing the HDI to pre-POC molar ratio resulted in a significant increase in elasticity with an elongation at break of 129.58 ± 32.99%, 187.22 ± 26.78% ($p < 0.05$), and 257.60 ± 8.51% ($p < 0.01$) for CUPE 1.2, 1.5, and 1.8, respectively. To determine the affect of the total channel number on the resulting scaffold mechanical strength, various CUPE scaffolds with total channel numbers ranging from 1-5 were evaluated for tensile peak stress. Interestingly, it was observed that no significant difference ($p > 0.05$) in peak stress was observed as the total number of channels was increased (Fig. 6).

Multichanneled CUPE TENG *in vivo* evaluation

Various nerve conduits were also evaluated *in vivo* to repair a 1 cm rat sciatic nerve defect. Figures 7-8 show microscopic images of five sections taken throughout the guides stained with H&E (Fig. 7) and Toluidine blue (Fig. 8) following 8 weeks of implantation. The proximal nerves for all groups were normal in appearance consisting of myelinated axons, large amounts of axon bundles, and the presence of fascicles. Tissue infiltration can be seen throughout the interior of all the conduits tested. However, very minimal tissue infiltration was observed in the central conduit sections of the PCL hollow tubes. H&E stained sections also show that the multichanneled CUPE TENGs were unable to maintain channel integrity (Fig. 7). Other than the PCL hollow tube, which showed nearly disconnected neural tissue, the myelinated axons were evenly distributed at the central conduit for both the nerve autograft and multichanneled CUPE TENGs. When comparing the neural fiber patterns, the CUPE TENGs showed a similar structure as that in the nerve autograft in terms of the myelinated fiber density and population ($p > 0.05$). Table 1 summarizes the average fiber

NIH-PA Author Manuscript

NIH-PA Author Manuscript

NIH-PA Author Manuscript

population, fiber density within 0.01 mm^2 of sections, and the average fiber diameter in the central conduits of CUPE TENGs, nerve autograft, and PCL hollow tubes. Among these groups, the CUPE guides displayed the most dense fiber population (12,914 ± 2454 mm^2). A similar fiber population and density to the nerve autograft was seen ($p > 0.05$), but was significantly different from those in the PCL tube ($p < 0.05$). However, the fiber diameter in CUPE scaffold was relatively smaller than that measured in the nerve autograft ($p > 0.05$).

DISCUSSION

Despite the significant advancements in the development of complex scaffolding for tissue engineering, the current clinical gold standard for peripheral nerve repair has not changed for over 30 years.[2,26-30] To date, no other repair strategy has been able to offer the advantages which autologous nerve grafts provide.[15] Although a variety materials and scaffold fabrication methods have been investigated as potential autologous nerve graft replacements, the use of a single hollow tube based upon an entubulation model as a conduit for neural regeneration has shown limited success.[31-33] Recent research has indicated that the scaffold microarchitectural and mechanical characteristics are important factors in controlling factors related to the overall success of the implant including cell orientation, tissue organization/architecture, rate of neotissue formation, and ability of the implant to integrate with native tissue.[34-36] In response to the biomimetic microarchitectural requirements for nerve regeneration, it is hypothesized that recreating the native tissue architecture at the macro-, micro-, and nano-scales can facilitate cell and extracellular matrix compartmentalization to engineer a more native-like and functional nerve.[17,37-39] For peripheral nerve regeneration, it is important that the TENG be mechanically compliant and contain an array of parallel and longitudinally oriented microchannels to replicate the native basal lamina.[2,29,40-42] Through the use of multichanneled designs, an improvement in nerve target reinnervation, increase in surface area for cell growth, and the ability to provide the necessary anisotropic physical cues to direct the growth of regenerating nerve fibers can be accomplished.[6,15]

To address these major requirements, we have reported the fabrication and characterization of soft, elastic, and strong multichanneled CUPE TENG for peripheral nerve regeneration with the following advantages over previous designs (Fig. 1): 1) The use of a strong, elastic, and biocompatible biomaterial may reduce the compliance mismatch between the graft and host tissue, which is a biomechanical problem that has been well documented as a factor of implant failure.[43,44] CUPE is a strong, soft, and highly elastic biodegradable citrate-based polymer developed in our lab and was chosen as the biomaterial for guide fabrication due to its biocompatibility, hemocompatibility, controlled degradation (few weeks to more than a year), and suitable soft tissue mechanical properties, which can be adjusted through the monomer ratios, choices of monomers, and post-polymerization conditions.[23] This is the first reported application of CUPE for neural tissue engineering, and it is expected that a nerve guide fabricated using CUPE can potentially maintain adequate guide strength, elasticity, withstand tension, and retain sutures upon pore introduction. 2) The parallel multichannel design can better mimic the native architecture of nerve basal lamina tubes and promote nerve cell alignment through contact guidance; 3) To impart porosity into the grafts, we chose to use particulate leaching technique, which is a simple, cost-effective

NIH-PA Author Manuscript

NIH-PA Author Manuscript

NIH-PA Author Manuscript

scaffold fabrication method that can be applied to a wide range of biomaterials; 4) The introduction of microporosity (<10 μm) between the channels can potentially minimize fibrous tissue infiltration, increase permeability for cell-to-cell communication, and limit cell dispersion to enhance nerve target reinnervation; and 5) The outer sheath of the nerve guide conduit can provide a suitable surface for surgical implantation via suturing and the necessary scaffold mechanical strength for dynamic environments *in vivo*. We have based the fabrication of the biomimetic TENGs using a micro-engineering approach pioneered in 2006 by Wang et al., who ingeniously utilized acupuncture needles as a mandrel to define the longitudinally aligned microchannels within the guide.[16] Acupuncture needles are highly resistant to corrosion, uniform in size, and are commercially availability in various diameters ranging from 140 to 500 μm.[2] The acupuncture needle length ultimately determines the resulting guide length; however it should be noted that a majority of the commercially available needles are a minimum of 4 cm in length and longer needles can be applied to fabricate TENGs for use in significant gap length repair. In this study, CUPE TENGs with channel numbers ranging from 1-5 were fabricated using the current molds. One major advantage of this approach is that the number, diameter, and spatial distribution of the channels can be finely controlled through computer-aided design to produce novel scaffolding for nerve regeneration in accordance with the parameters of future studies, which will be aimed at studying the effects of channel number, channel size, and porosity on peripheral nerve regeneration.

Sequential slices throughout the length of the CUPE TENGs showed the ability of the acupuncture needles to retain a well-defined parallel orientation of each channel throughout the length of the guide, and cross-sections throughout the length of the guide had almost the same transverse morphology to indicate a continuous microchanneled design. The SEM images in Figure 3 and 4 show the circular uniformity of each individual channel, which was designed to replicate the basal lamina of native nerves. A simple and cost-effective, NaCl particulate leaching technique was used herein to produce highly porous and interconnected regions in between the channels, and upon further inspection, SEM images revealed a luminal submicron topography inside each channel, which can potentially aid in cell communication and nutrient/waste exchange (Fig. 3C). As nerve regeneration requires an orchestrated combinational response of matrix topography and secreted cellular signals, the porous matrix fabricated in this study can potentially enhance peripheral nerve regeneration relative to impermeable conduits.[8] The size of the pores were chosen to be approximately 10 μm in order to potentially maintain a permeable matrix for metabolite transport while minimizing the possibility for cell migration in between individual channels to promote proper target reinnervation.[38,45,46] Figure 3A shows a well-integrated non-porous outer sheath, which was incorporated into the guide design to provide mechanical support for increased suture retention strengths and potentially aid in the prevention of fibrous tissue infiltration into the guide. Future studies will be focused on additional compressive mechanical testing and permeability assessment on nerve guides with semi-porous outer sheaths ranging from 0-50% porosity, which may have the ability to balance the mechanical strength while also allowing for nutrient exchange and potential guide vascularization.

NIH-PA Author Manuscript

NIH-PA Author Manuscript

NIH-PA Author Manuscript

Native nerves are strong and elastic in nature with ultimate tensile stress values of 1.11 – 3.69 MPa, initial modulus of 0.42 – 0.73 MPa, and elongations at break between 48 – 81%.[47] The reported values of multichanneled CUPE TENGs developed herein were in accordance to the values of native nerves. Previous guide designs for nerve tissue engineering have been primarily focused on the use of stiff and inelastic biodegradable materials. The mismatch in compliance often leads to increased scar tissue formation at the implant/tissue interface, and causes implant failure in mechanically dynamic environments where constant movement, tension, and elasticity are encountered.[48] The CUPE TENGs fabricated in this study were strong and highly elastic as shown in Figure 5 and can be fine-tuned through monomer ratios, HDI concentration, and post-polymerization conditions to cover a wide range of parameters.[49] Figure 5C shows that the tested TENGs displayed suture retention strengths of up to 2.4 ± 0.12 N, which exceed the surgical requirement of 1.6 N.[48] To determine the affect of the total channel number on the resulting scaffold mechanical strength, various CUPE scaffolds with total channel numbers ranging from 1-5 were evaluated for tensile peak stress. Interestingly, it was observed that no significant difference ($p > 0.05$) in peak stress was observed as the total number of channels was increased (Fig. 6). This observation indicates that the mechanical strength of the scaffolds was primarily due to the presence of the outer film.

In addition to mechanical testing, the fabricated CUPE TENGs were compared with PCL hollow tubes and nerve autografts *in vivo* using a 1 cm rat sciatic nerve defect model to determine their ability to regenerate peripheral nerve. PCL hollow tubes were fabricated with similar outer diameters to that of the CUPE TENGs, and CUPE 1.5 crosslinked at 80-4 + 120-1 were selected for implantation due to balance between strength and elasticity. Upon implantation of the implants, it was observed that suturing of the CUPE TENGs was easily accomplished with no dislocation of the samples to the native nerve stumps due to the presence of the solid, non-porous outer sheath. In addition, both the outer sheath and inner nerve stump were well integrated and absent of any gaps. Although, the CUPE TENGs showed comparable results with that of nerve autografts and outperformed hollow tubes in terms of fiber population and densities, this work was unfortunately limited by the lack of functional evaluation and maintenance of guide structure throughout the animal study. Microscopic images from thin sections (Fig. 7) revealed collapse of the inner structure from CUPE TENGs after eight weeks implantation, which could be due to a variety of factors. The micro-architecture of CUPE TENGs was not preserved in the animal hind limb possibly due to the vigorous movement of the rats, or inadequate mechanical properties of the conduits used for implantation. Since movement from the animal cannot be controlled, improvements should be focused on the architecture and mechanical properties of the guide. For example, reducing the diameter of the channels, which would provide additional scaffolding material in between channels, can be one potential strategy for future improvements. Previous studies have shown that the diameter of human myelinated nerve fiber is smaller than 20 μm,[6] and guides fabricated with smaller diameter channels can increase axonal regeneration over larger diameter channels.[20] In addition to optimizing the scaffold geometry, scaffold strength can also be enhanced with increased CUPE HDI ratios. CUPE TENGs implanted in this study were fabricated from CUPE synthesized using 1.5

NIH-PA Author Manuscript

NIH-PA Author Manuscript

NIH-PA Author Manuscript

HDI molar ratios, and it is feasible that increased HDI ratios in combination with improved channel diameters may provide adequate strength to prevent future collapse.

Therefore, future studies will be focused on optimizing guide parameters with special consideration taken on compressive strength to improve perigraft tissue compression from muscle contraction, joint movement, and body weight.[6] In addition, functional analysis (i.e. electrophysiology and motion analysis) will be included to provide a better understanding of the tissue types present and improve our knowledge of the guide performance. The obtained results do, however, provide valuable information on the necessary future scaffold design improvements needed and merit further investigation on strategies to incorporate additional biological factors. It is worthy to note that the *in vivo* results presented above on sciatic nerve regeneration were based on naked CUPE TENGs without any supplements or growth factors. Intensive studies have shown that a myriad of growth factors can promote nerve regeneration including nerve growth factor (NGF), neurotrophin-3 (NT-3), glial cell-derived neurotrophic factor (GDNF), fibroblast growth factor (FGF), ciliary neurotrophic factor (CNTF), glial growth factor (GGF), vascular endothelial growth factor (VEGF), brain-derived neurotrophic factor (BDNF), leukemia inhibitory factor (LIF), insulin-like growth factor 1 (IGF-1), and platelet-derived growth factor (PDGF).[45,50-53] Whether the incorporation of a single growth factor or a cocktail of factors to potentially improve the regenerative capabilities of CUPE TENGs remains to be seen. However, these are the first steps towards realizing the ultimate goal of this work, which is to create an off-the-shelf TENG ready for immediate implantation and circumvent lengthy *in vitro* cell culture requirements.

CONCLUSIONS

In conclusion, porous, elastic, and biomimetic CUPE TENGs consisting of parallel and longitudinally oriented microchannels and a non porous outer sheath to guide the outgrowth of nerve fibers and prevent the ingrowth of fibrous tissue in the nerve gap, respectively, were fabricated for peripheral nerve regeneration using a simple and cost-effective sodium chloride particulate leaching technique in combination with micro-engineering approaches. Using this design, microfabricated TENGs can be produced with tunable architectural geometries and strength. The resulting conduits were evaluated based on their geometry, mechanical properties, and *in vivo* performance. Although further improvements must be made in scaffold geometry to prevent future collapse, these studies represent the first step toward the investigation of the role of CUPE scaffold architecture on the resulting tensile, suture retention, and *in vivo* performance. It is our belief that the CUPE TENGs could potentially serve as off-the-shelf nerve conduits for peripheral nerve regeneration.

Acknowledgments

This work was partially supported by a R01 award (EB012575) from the National Institute of Biomedical Imaging and Bioengineering (NIBIB), a National Science Foundation (NSF) CAREER award (1313553), and a NSF collaborative research award (CMMI 1266116).

Authors' roles: Study design: WKI, KWKY, and JY. Study conduct: RTT, WMC, HC, and IQ. Data collection: RTT, WMC, and IQ. Data analysis: RTT, WMC, KWKY, and JY. Data interpretation: RTT, WMC, KWKY, and

NIH-PA Author Manuscript

NIH-PA Author Manuscript

NIH-PA Author Manuscript

JY. Drafting manuscript: RTT. Revising manuscript content: RTT and JY. Approving final version of manuscript: WKI, KWKY, JCC, and JY. KWKY and JY take responsibility for the integrity of the data analysis.

REFERENCES

1. Bryan DJ, Tang JB, Doherty SA, Hile DD, Trantolo DJ, Wise DL, Summerhayes IC. Enhanced peripheral nerve regeneration through a poled bioresorbable poly(lactic-co-glycolic acid) guidance channel. J Neural Eng. 2004; 1(2):91–8. [PubMed: 15876627]
2. Bozkurt A, Brook GA, Moellers S, Lassner F, Sellhaus B, Weis J, Woeltje M, Tank J, Beckmann C, Fuchs P. In vitro assessment of axonal growth using dorsal root ganglia explants in a novel three-dimensional collagen matrix. Tissue Eng. 2007; 13(12):2971–9. others. [PubMed: 17937537]
3. Guenard V, Kleitman N, Morrissey TK, Bunge RP, Aebischer P. Syngeneic Schwann cells derived from adult nerves seeded in semipermeable guidance channels enhance peripheral nerve regeneration. J Neurosci. 1992; 12(9):3310–20. [PubMed: 1527582]
4. Jacobs WB, Fehlings MG. The molecular basis of neural regeneration. Neurosurgery. 2003; 53(4): 943–48. discussion 948-50. [PubMed: 14519226]
5. Bender MD, Bennett JM, Waddell RL, Doctor JS, Marra KG. Multi-channeled biodegradable polymer/CultiSpher composite nerve guides. Biomaterials. 2004; 25(7-8):1269–78. [PubMed: 14643601]
6. Ao Q, Wang A, Cao W, Zhang L, Kong L, He Q, Gong Y, Zhang X. Manufacture of multimicrotubule chitosan nerve conduits with novel molds and characterization in vitro. J Biomed Mater Res A. 2006; 77(1):11–8. [PubMed: 16345091]
7. Flynn L, Dalton PD, Shoichet MS. Fiber templating of poly(2-hydroxyethyl methacrylate) for neural tissue engineering. Biomaterials. 2003; 24(23):4265–72. [PubMed: 12853258]
8. Huang YC, Huang YY, Huang CC, Liu HC. Manufacture of porous polymer nerve conduits through a lyophilizing and wire-heating process. J Biomed Mater Res B Appl Biomater. 2005; 74(1):659–64. [PubMed: 15909301]
9. Dubey N, Letourneau PC, Tranquillo RT. Guided neurite elongation and schwann cell invasion into magnetically aligned collagen in simulated peripheral nerve regeneration. Exp Neurol. 1999; 158(2):338–50. [PubMed: 10415141]
10. Rangappa N, Romero A, Nelson KD, Eberhart RC, Smith GM. Laminin-coated poly(L-lactide) filaments induce robust neurite growth while providing directional orientation. J Biomed Mater Res. 2000; 51(4):625–34. [PubMed: 10880110]
11. Terada N, Bjursten LM, Papaloizos M, Lundborg G. Resorbable filament structures as a scaffold for matrix formation and axonal growth in bioartificial nerve grafts: long term observations. Restor Neurol Neurosci. 1997; 11(1):65–9. [PubMed: 21551529]
12. Wang S, Wan AC, Xu X, Gao S, Mao HQ, Leong KW, Yu H. A new nerve guide conduit material composed of a biodegradable poly(phosphoester). Biomaterials. 2001; 22(10):1157–69. [PubMed: 11352095]
13. Stevenson TR, Kadhiresan VA, Faulkner JA. Tubular nerve guide and epineurial repair: comparison of techniques for neurorrhaphy. J Reconstr Microsurg. 1994; 10(3):171–4. [PubMed: 8071904]
14. Sundback C, Hadlock T, Cheney M, Vacanti J. Manufacture of porous polymer nerve conduits by a novel low-pressure injection molding process. Biomaterials. 2003; 24(5):819–30. [PubMed: 12485800]
15. Hadlock T, Sundback C, Hunter D, Cheney M, Vacanti JP. A polymer foam conduit seeded with Schwann cells promotes guided peripheral nerve regeneration. Tissue Eng. 2000; 6(2):119–27. [PubMed: 10941207]
16. Wang A, Ao Q, Cao W, Yu M, He Q, Kong L, Zhang L, Gong Y, Zhang X. Porous chitosan tubular scaffolds with knitted outer wall and controllable inner structure for nerve tissue engineering. J Biomed Mater Res A. 2006; 79(1):36–46. [PubMed: 16758450]
17. Lu Q, Simionescu A, Vyavahare N. Novel capillary channel fiber scaffolds for guided tissue engineering. Acta Biomater. 2005; 1(6):607–14. [PubMed: 16701841]

NIH-PA Author Manuscript

NIH-PA Author Manuscript

NIH-PA Author Manuscript

18. Brayfield CA, Marra KG, Leonard JP, Tracy Cui X, Gerlach JC. Excimer laser channel creation in polyethersulfone hollow fibers for compartmentalized in vitro neuronal cell culture scaffolds. Acta Biomater. 2008; 4(2):244–55. [PubMed: 18060849]
19. Zhang M, Yannas IV. Peripheral nerve regeneration. Adv Biochem Eng Biotechnol. 2005; 94:67–89. [PubMed: 15915869]
20. Krych AJ, Rooney GE, Chen B, Schermerhorn TC, Ameenuddin S, Gross L, Moore MJ, Currier BL, Spinner RJ, Friedman JA. Relationship between scaffold channel diameter and number of regenerating axons in the transected rat spinal cord. Acta Biomater. 2009; 5(7):2551–9. others. [PubMed: 19409869]
21. Hu X, Huang J, Ye Z, Xia L, Li M, Lv B, Shen X, Luo Z. A novel scaffold with longitudinally oriented microchannels promotes peripheral nerve regeneration. Tissue Eng Part A. 2009; 15(11): 3297–308. [PubMed: 19382873]
22. Li J, Rickett TA, Shi R. Biomimetic nerve scaffolds with aligned intraluminal microchannels: a “sweet” approach to tissue engineering. Langmuir. 2009; 25(3):1813–7. [PubMed: 19105786]
23. Dey J, Xu H, Shen J, Thevenot P, Gondi SR, Nguyen KT, Sumerlin BS, Tang L, Yang J. Development of biodegradable crosslinked urethane-doped polyester elastomers. Biomaterials. 2008; 29(35):4637–49. [PubMed: 18801566]
24. Yang J, Shi G, Bei J, Wang S, Cao Y, Shang Q, Yang G, Wang W. Fabrication and surface modification of macroporous poly(L-lactic acid) and poly(L-lactic-co-glycolic acid) (70/30) cell scaffolds for human skin fibroblast cell culture. J Biomed Mater Res. 2002; 62(3):438–46. [PubMed: 12209930]
25. Lee SJ, Oh SH, Liu J, Soker S, Atala A, Yoo JJ. The use of thermal treatments to enhance the mechanical properties of electrospun poly(epsilon-caprolactone) scaffolds. Biomaterials. 2008; 29(10):1422–30. [PubMed: 18096219]
26. Lundborg G. A 25-year perspective of peripheral nerve surgery: evolving neuroscientific concepts and clinical significance. J Hand Surg Am. 2000; 25(3):391–414. [PubMed: 10811744]
27. Sparmann M. Orthopade. 1998; 27(7):433–40. [Nerve prosthesis. Current status]. [PubMed: 9728352]
28. Yannas IV, Hill BJ. Selection of biomaterials for peripheral nerve regeneration using data from the nerve chamber model. Biomaterials. 2004; 25(9):1593–600. [PubMed: 14697861]
29. Stang F, Fansa H, Wolf G, Reppin M, Keilhoff G. Structural parameters of collagen nerve grafts influence peripheral nerve regeneration. Biomaterials. 2005; 26(16):3083–91. [PubMed: 15603803]
30. Ciardelli G, Chiono V. Materials for peripheral nerve regeneration. Macromol Biosci. 2006; 6(1): 13–26. [PubMed: 16374766]
31. Chalfoun CT, Wirth GA, Evans GR. Tissue engineered nerve constructs: where do we stand? J Cell Mol Med. 2006; 10(2):309–17. [PubMed: 16796801]
32. Jeffries EM, Wang Y. Biomimetic micropatterned multi-channel nerve guides by templated electrospinning. Biotechnol Bioeng. 2012; 109(6):1571–82. [PubMed: 22179932]
33. Panseri S, Cunha C, Lowery J, Del Carro U, Taraballi F, Amadio S, Vescovi A, Gelain F. Electrospun micro- and nanofiber tubes for functional nervous regeneration in sciatic nerve transections. BMC Biotechnol. 2008; 8:39. [PubMed: 18405347]
34. Bozkurt A, Deumens R, Beckmann C, Olde Damink L, Schugner F, Heschel I, Sellhaus B, Weis J, Jahnen-Dechent W, Brook GA. In vitro cell alignment obtained with a Schwann cell enriched microstructured nerve guide with longitudinal guidance channels. Biomaterials. 2009; 30(2):169–79. others. [PubMed: 18922575]
35. Moore MJ, Friedman JA, Lewellyn EB, Mantila SM, Krych AJ, Ameenuddin S, Knight AM, Lu L, Currier BL, Spinner RJ. Multiple-channel scaffolds to promote spinal cord axon regeneration. Biomaterials. 2006; 27(3):419–29. others. [PubMed: 16137759]
36. Tran RT, Naseri E, Kolasnikov A, Bai X, Yang J. A new generation of sodium chloride porogen for tissue engineering. Biotechnol Appl Biochem. 2011; 58(5):335–44. [PubMed: 21995536]
37. Sun C, Jin X, Holzwarth JM, Liu X, Hu J, Gupte MJ, Zhao Y, Ma PX. Development of channeled nanofibrous scaffolds for oriented tissue engineering. Macromol Biosci. 2012; 12(6):761–9. [PubMed: 22508530]

NIH-PA Author Manuscript

NIH-PA Author Manuscript

NIH-PA Author Manuscript

38. Bozkurt A, Lassner F, O'Dey D, Deumens R, Bocker A, Schwendt T, Janzen C, Suschek CV, Tolba R, Kobayashi E. The role of microstructured and interconnected pore channels in a collagen-based nerve guide on axonal regeneration in peripheral nerves. Biomaterials. 2012; 33(5): 1363–75. others. [PubMed: 22082619]
39. de Ruiter GC, Onyeneho IA, Liang ET, Moore MJ, Knight AM, Malessy MJ, Spinner RJ, Lu L, Currier BL, Yaszemski MJ. Methods for in vitro characterization of multichannel nerve tubes. J Biomed Mater Res A. 2008; 84(3):643–51. others. [PubMed: 17635012]
40. Keilhoff G, Stang F, Wolf G, Fansa H. Bio-compatibility of type I/III collagen matrix for peripheral nerve reconstruction. Biomaterials. 2003; 24(16):2779–87. [PubMed: 12711525]
41. Lietz M, Dreesmann L, Hoss M, Oberhoffner S, Schlosshauer B. Neuro tissue engineering of glial nerve guides and the impact of different cell types. Biomaterials. 2006; 27(8):1425–36. [PubMed: 16169587]
42. Sinis N, Schaller HE, Schulte-Eversum C, Schlosshauer B, Doser M, Dietz K, Rosner H, Muller HW, Haerle M. Nerve regeneration across a 2-cm gap in the rat median nerve using a resorbable nerve conduit filled with Schwann cells. J Neurosurg. 2005; 103(6):1067–76. [PubMed: 16381194]
43. Yang J, Motlagh D, Webb AR, Ameer GA. Novel biphasic elastomeric scaffold for small-diameter blood vessel tissue engineering. Tissue Eng. 2005; 11(11-12):1876–86. [PubMed: 16411834]
44. Tran RT, Thevenot P, Gyawali D, Chiao JC, Tang L, Yang J. Synthesis and characterization of a biodegradable elastomer featuring a dual crosslinking mechanism. Soft Matter. 2010; 6(11):2449–2461. [PubMed: 22162975]
45. Schmidt CE, Leach JB. Neural tissue engineering: strategies for repair and regeneration. Annu Rev Biomed Eng. 2003; 5:293–347. [PubMed: 14527315]
46. Stokols S, Tuszynski MH. The fabrication and characterization of linearly oriented nerve guidance scaffolds for spinal cord injury. Biomaterials. 2004; 25(27):5839–46. [PubMed: 15172496]
47. Borschel GH, Kia KF, Kuzon WM Jr. Dennis RG. Mechanical properties of acellular peripheral nerve. J Surg Res. 2003; 114(2):133–9. [PubMed: 14559438]
48. Tran RT, Thevenot P, Zhang Y, Gyawali D, Tang L, Yang J. Scaffold Sheet Design Strategy for Soft Tissue Engineering. Nat Mater. 2010; 3(2):1375–1389. [PubMed: 21113339]
49. Dey J, Tran RT, Shen J, Tang L, Yang J. Development and long-term in vivo evaluation of a biodegradable urethane-doped polyester elastomer. Macromol Mater Eng. 2011; 296(12):1149–1157. [PubMed: 22184499]
50. Babensee JE, McIntire LV, Mikos AG. Growth factor delivery for tissue engineering. Pharm Res. 2000; 17(5):497–504. [PubMed: 10888299]
51. Whitaker MJ, Quirk RA, Howdle SM, Shakesheff KM. Growth factor release from tissue engineering scaffolds. J Pharm Pharmacol. 2001; 53(11):1427–37. [PubMed: 11732745]
52. Lee K, Silva EA, Mooney DJ. Growth factor delivery-based tissue engineering: general approaches and a review of recent developments. J R Soc Interface. 2011; 8(55):153–70. [PubMed: 20719768]
53. Bryan DJ, Holway AH, Wang KK, Silva AE, Trantolo DJ, Wise D, Summerhayes IC. Influence of glial growth factor and Schwann cells in a bioresorbable guidance channel on peripheral nerve regeneration. Tissue Eng. 2000; 6(2):129–38. [PubMed: 10941208]

NIH-PA Author Manuscript

NIH-PA Author Manuscript

NIH-PA Author Manuscript

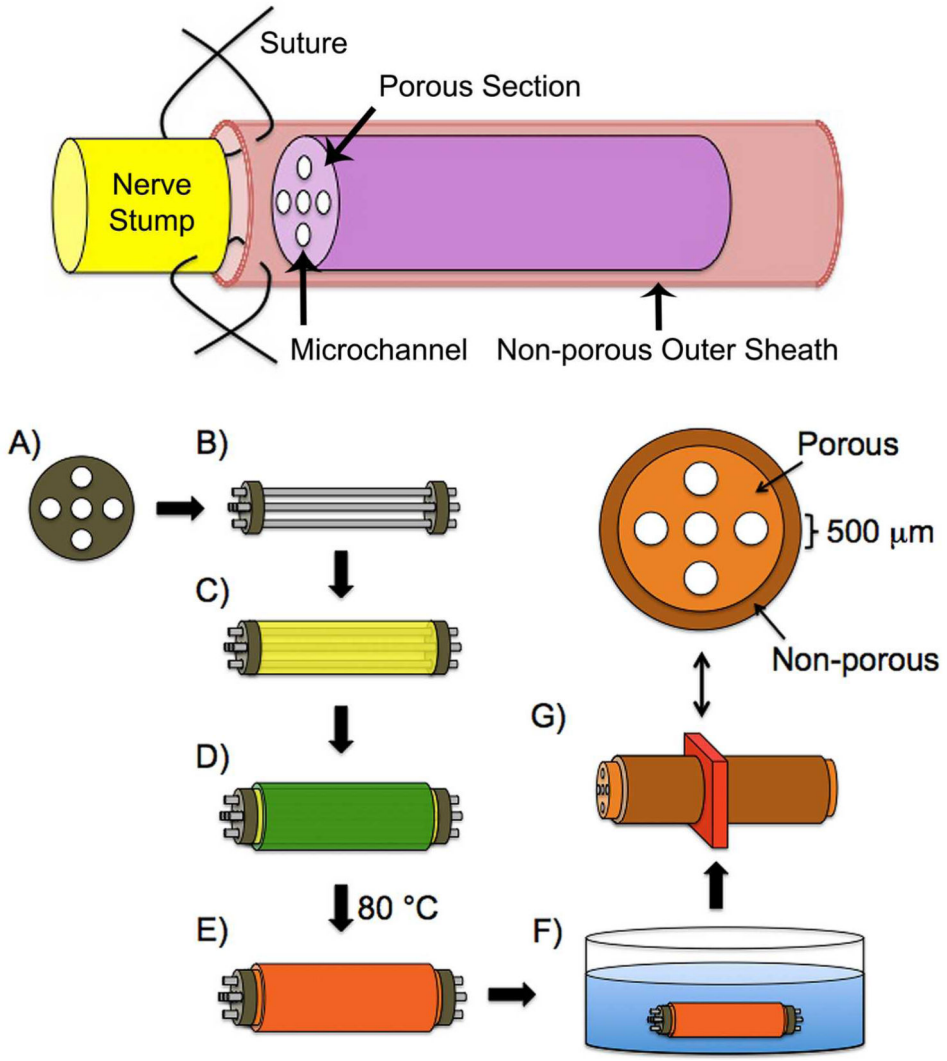

FIGURE 1.

Schematic illustration of an elastic, porous, and longitudinally aligned multichanneled crosslinked urethane-doped polyester (CUPE) tissue engineered nerve guide for attaching the proximal and distal ends of severed peripheral nerves via sutures and guide fabrication process. A titanium shim is first microengineered using computer-automated design (A) followed by the insertion of acupuncture needles through two titanium shims (B). Next, a pre-CUPE and NaCl mixture is cast in between the acupuncture needles (C) followed by dip coating the guide in pre-CUPE to form the non-porous outer sheath (D). The entire construct is then post-polymerized under various conditions (E) followed by NaCl porogen removal in deionized water (F). Representative CUPE nerve guide cross-section indicating channel diameters, porous, and non-porous regions (G).

NIH-PA Author Manuscript

NIH-PA Author Manuscript

NIH-PA Author Manuscript

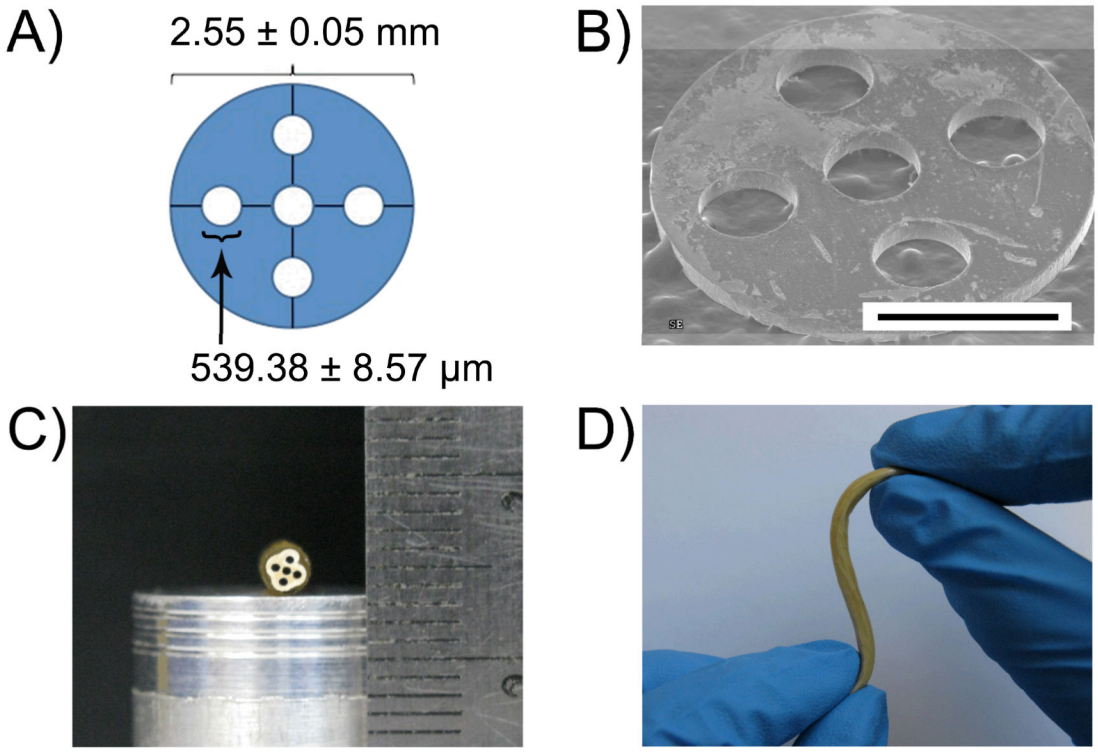

FIGURE 2.

A) Design and geometry of titanium shims and B) overall scanning electron microscope (SEM) image (scale bar 1 mm). C) Multichanneled crosslinked-urethane doped polyester (CUPE) tissue engineered nerve guide cross-section photograph and D) multidirectional bend without kinks to show soft and elastic nature of the material.

NIH-PA Author Manuscript

NIH-PA Author Manuscript

NIH-PA Author Manuscript

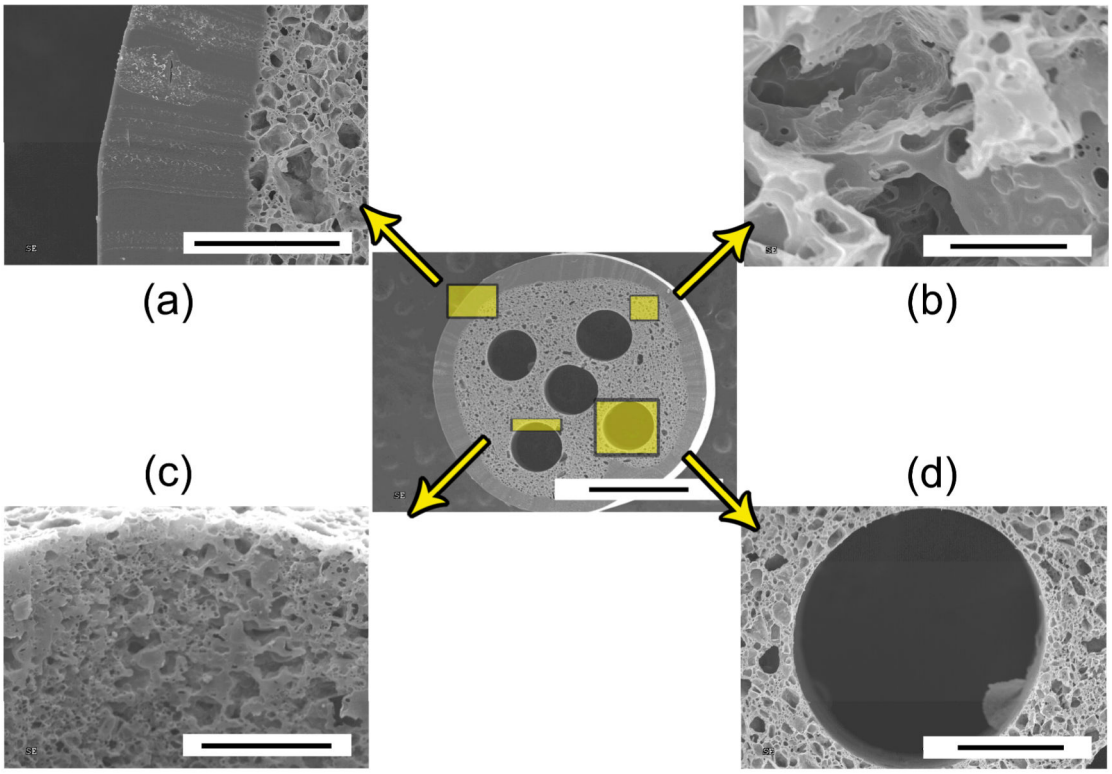

FIGURE 3.

Scanning election microscope (SEM) images of porous and elastic multichanneled crosslinked urethane-doped polyester (CUPE) tissue engineered nerve guide cross-section (center; scale bar = 1 mm), (a) outer sheath (scale bar = 200 μm), (b) representative porous section (scale bar = 20 μm), (c) channel lumen porosity and topography (scale bar = 100 μm), and (d) channel diameter (scale bar = 200 μm).

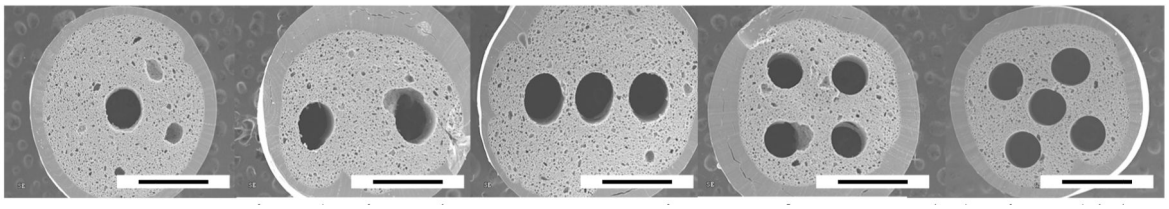

FIGURE 4.

Scanning election microscope (SEM) images of porous and elastic multichanneled crosslinked urethane-doped polyester (CUPE) tissue engineered nerve guide fabricated with various channel numbers (scale bar = 1 mm).

NIH-PA Author Manuscript
NIH-PA Author Manuscript
NIH-PA Author Manuscript

NIH-PA Author Manuscript

NIH-PA Author Manuscript

NIH-PA Author Manuscript

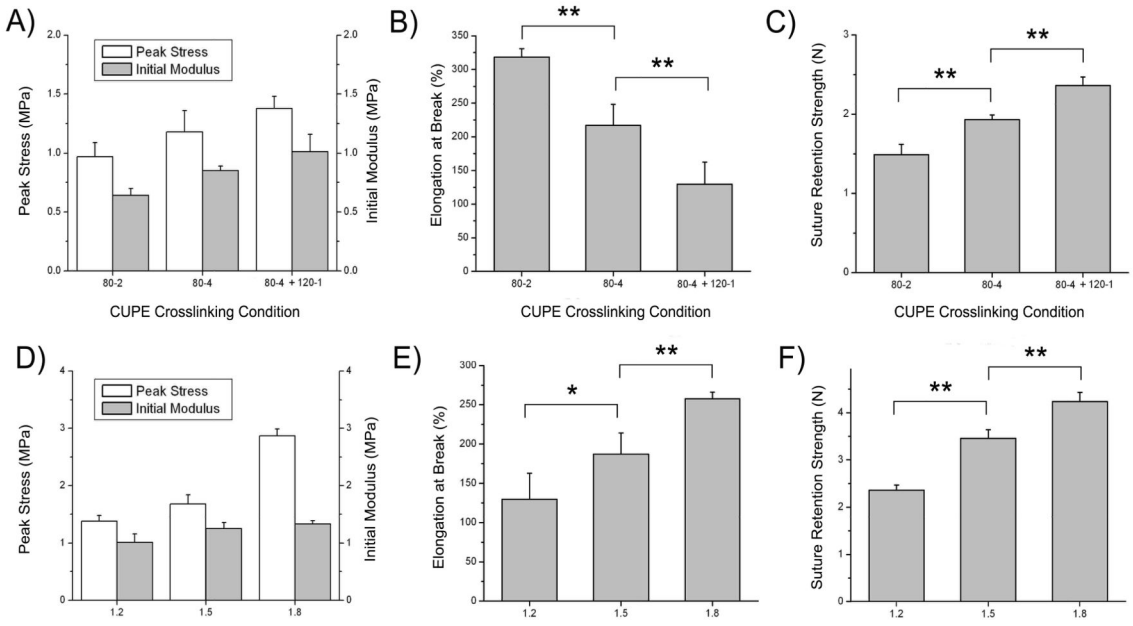

FIGURE 5.

The effects of various CUPE 1.2 crosslinking conditions on the resulting scaffold A) peak stress and initial modulus, B) elongation at break, and C) maximum suture retention strength. The effects of various CUPE diisocyanate ratios on the resulting guide D) peak stress and initial modulus, E) elongation at break, and F) maximum suture retention strength crosslinked at 80 °C for 4 days followed by 120 °C for one day. Values are reported as the mean ± standard deviation (n = 6; * indicates significant difference $p < 0.05$; ** indicates significant difference $p < 0.01$).

NIH-PA Author Manuscript

NIH-PA Author Manuscript

NIH-PA Author Manuscript

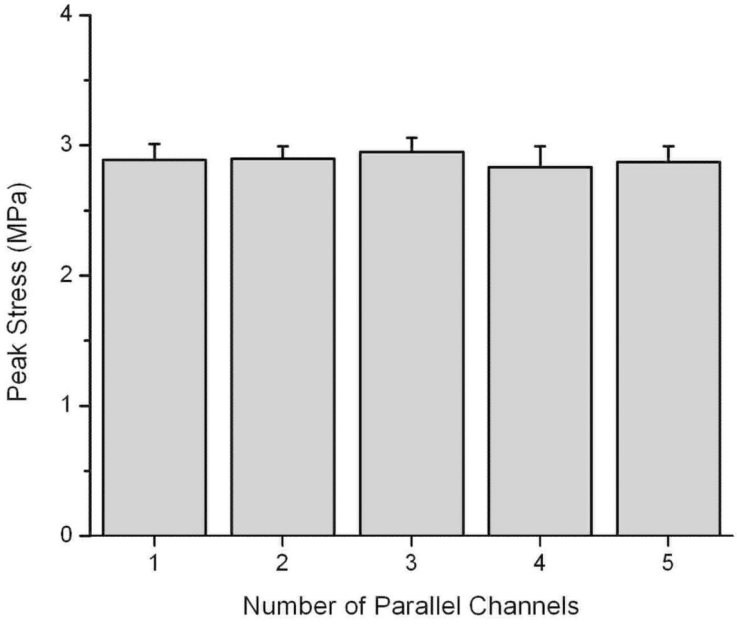

FIGURE 6.

The effect of channel number on porous and elastic multichanneled crosslinked urethane-doped polyester (CUPE) tissue engineered nerve guide tensile strength. (n = 6; mean ± standard deviation).

NIH-PA Author Manuscript

NIH-PA Author Manuscript

NIH-PA Author Manuscript

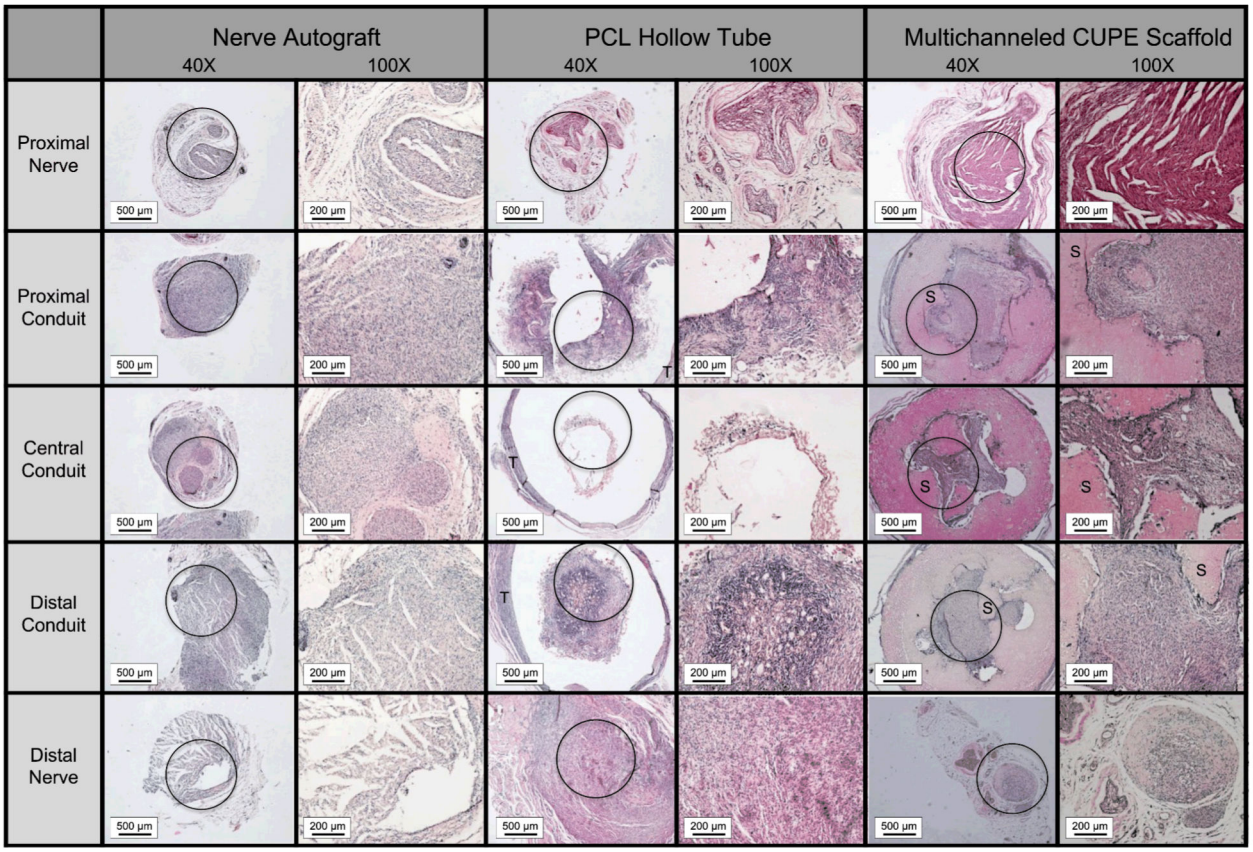

FIGURE 7.

Microscopic images (40× and 100×) of semi-thin cross sections of tissue explants stained with hematoxylin and eosin (H&E) through nerve autograft, poly (caprolactone) (PCL) hollow tube, and multichanneled crosslinked urethane-doped polyester (CUPE) tissue engineered nerve guides implanted to repair a 1 cm rat sciatic nerve defect (circle indicates area of 40× tissue section where 100× picture was recorded; T indicates location of PCL tube; S indicates location of CUPE nerve guide).

NIH-PA Author Manuscript

NIH-PA Author Manuscript

NIH-PA Author Manuscript

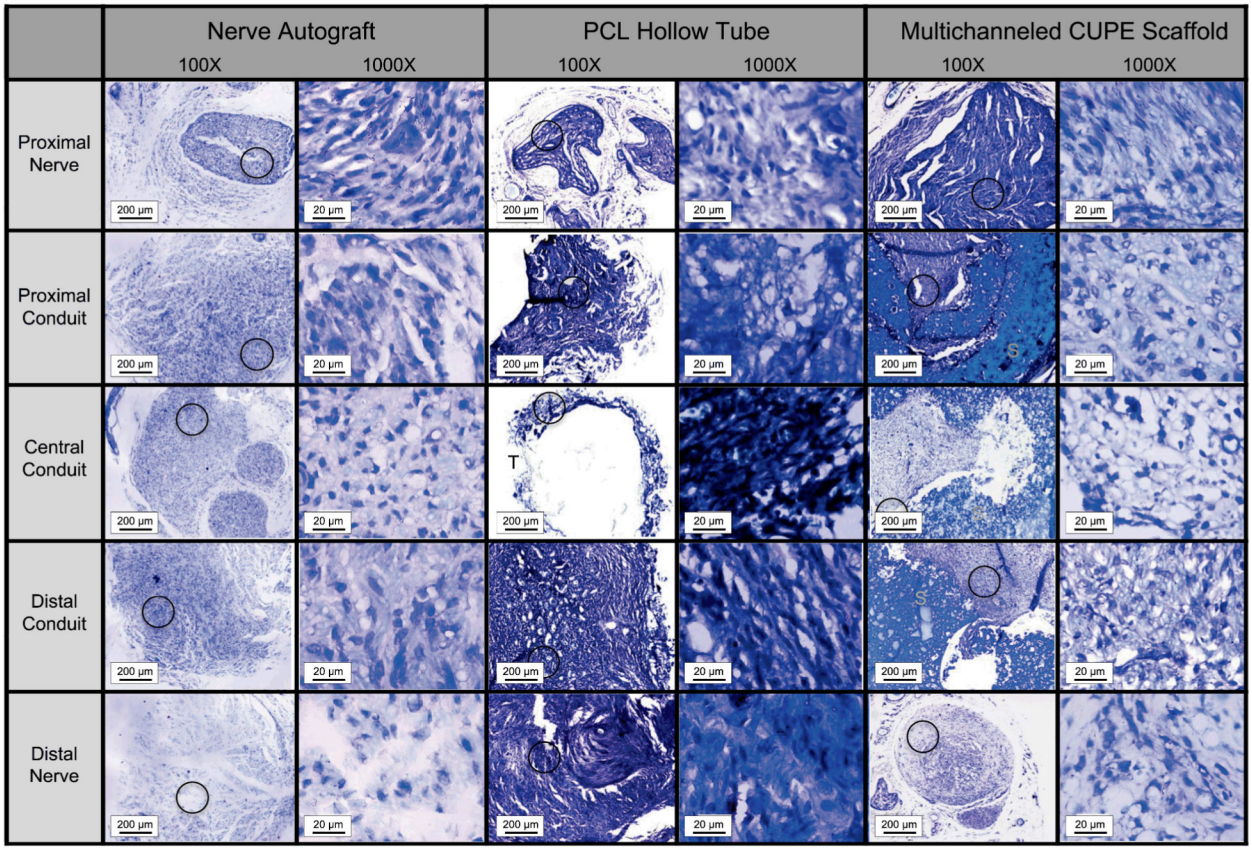

FIGURE 8.

Microscopic images (100× and 1000×) of semi-thin cross sections of tissue explants stained with toluidine blue through nerve autograft, poly (caprolactone) (PCL) hollow tube, and multichanneled crosslinked urethane-doped polyester (CUPE) tissue engineered nerve guides implanted to repair a 1 cm rat sciatic nerve defect (circle indicates area of 40× tissue section where 1000× picture was recorded; T indicates location of PCL tube; S indicates location of CUPE nerve guide).

NIH-PA Author Manuscript

NIH-PA Author Manuscript

NIH-PA Author Manuscript

TABLE 1

Summary of the nerve fiber population, density, and diameter in the central conduit of nerve autograft (control), poly (caprolactone) (PCL) hollow tube, and porous and elastic crosslinked urethane-doped polyester (CUPE) multichanneled scaffolds after 8 weeks of implantation to repair a 1 cm sciatic nerve defect rat model. [a]

Group	Fiber Population	Fiber Density (mm^2)	Fiber Diameter (μm)
Nerve Autograft	120 ± 26	10,872 ± 2,318	0.87 ± 0.16
PCL Hollow Tube	52 ±10*	4,655 ± 915*	0.85 ± 0.15
CUPE Multichanneled Scaffold	143 ± 27	12,914 ± 2454	0.78 ± 0.17

[a] Values are reported as the mean ± standard deviation.

* Indicates a significant difference from other groups ($p < 0.05$).